LCPM2019
Toulouse, France

Nanospacecraft Exploration of Asteroids by Collision and flyby Reconnaissance (NEACORE)

IAA-LCPM-19-05-06

Lewis Walker[1], **Cristian Greco**[2],**Marilena Di Carlo**[3], **Andrew Wilson**[4], **Lorenzo Ricciardi**[5], **Audrey Berquand**[6], **and Massimiliano Vasile**[7]
[1][2][3][4][5][6][7]*University of Strathclyde, Level 8 James Weir Building, 75 Montrose Street, Glasgow, G1 1XJ, {lewis.walker@strath.ac.uk, c.greco@strath.ac.uk, marilena.di-carlo@strath.ac.uk, andrew.r.wilson@strath.ac.uk, lorenzo.ricciardi@strath.ac.uk, audrey.berquand@strath.ac.uk, massimiliano.vasile@strath.ac.uk}*

ABSTRACT

The number of visited asteroids is low compared to the total number that exists. Only a few missions have ever had a close approach or rendezvous with NEAs to better understand them. Additionally, as most observations are made from Earth, the uncertainties in their orbital elements could be greatly reduced with closer range measurements, while also allowing for other physical quantities to be determined such as mass, albedo, dimensions, and surface features.

This concurrent design study acts as a feasibility study for a new concept of nanosatellite mission framework which is intended to allow reconnaissance of a large number of NEAs while minimizing cost. The presented mission framework consists of pairs of nanosatellites travelling together on multi-target flyby trajectories, and is designed to be flexible to suit many different target sets. One such set is presented in detail, however the methods used to find this set also generated many other possible multi flyby trajectories that could equally be launched.

1. Introduction

To date, over 20,000 Near-Earth Asteroids (NEAs) have been identified [2], some of which are classified as being potentially hazardous, meaning they could pose a threat to Earth in the near future. Despite this, the orbital elements and physical/chemical characteristics of the vast majority of these objects are only known to limited levels of accuracy, since only very few missions have targeted them. Nano-satellites, which provide a valid low-cost, scaleable alternative to traditional spacecraft [30], are beginning to attract attention for the purposes of asteroid exploration and reconnaissance [7,31], and other deep-space missions [32,33] with a few missions already in development such as NEA Scout [6] and M-ARGO. The recent success of the first interplanetary CubeSats, MarCO-A and MarCO-B demonstrated that miniaturized platforms have reached an adequate technology readiness level to operate beyond Earth orbit.

This paper presents a feasibility analysis for a new, scaleable NEA reconnaissance mission framework using low-thrust nanosatellite platforms. It also presents a detailed analysis of one specific trajectory and target set to which the framework could be applied. This work extends a previously successful study on NEOs reachability and payload feasibility [8]. The primary scientific goal of each spacecraft is to improve the knowledge of visited NEAs in terms of their orbital elements and physical features and properties. Trajectories aim to maximize the number of visited NEAs per launch (balanced with favoring larger asteroids), with the aim of the platform being a means of large scale NEA exploration.

The feasibility study for this concept was performed during a concurrent design challenge at the Concurrent and Collaborative Design Studio (CCDS) at the University of Strathclyde (Glasgow, UK). The mission was designed in collaboration with CNES, and the outcome of the study is relevant to current efforts in SMPAG to define precursor missions.

2. Mission Framework

The mission concept is built around developing a low-cost framework for large-scale reconnaissance of large numbers of NEAs. In order to achieve this we aimed to create a single spacecraft design which could be produced on large scales in order to reduce development and production costs, while maximizing the scientific return. Each satellite would carry a low-thrust propulsion system with enough delta-V to make the necessary trajectory adjustments to fly by multiple targets in a single launch. These satellites are intended to fly by their targets at high velocity while still being able to take measurements, allowing a wider range of targets to be investigated.

A dedicated launcher would deliver a number of these satellites into LEO (reducing cost-per-spacecraft) attached to a 'kick stage', which would have sufficient delta-V to escape the Earth's sphere of influence. Once the kick stage is on an interplanetary trajectory, pairs of satellites would be deployed at specific times, each using low-thrust propulsion to embark on their respective multi-target trajectories. During the approach, final trajectory correction and measurement phases, spacecraft will operate autonomously. After each flyby event, the involved satellites would transmit the gathered data and cruise to the next burn point and subsequent target.

We expect a significantly reduced cost per satellite (and per explored asteroid) to conventional mission architectures, with the inclusion of a significant profit margin for the organizing body based on the sale of these craft to interested parties who would be able to choose targets and trajectories and receive all data gathered.

3. Mission Requirements

Req ID	Statement
MIS-1	The platform shall be flexible and tailorable to different flybys mission scenarios.
MIS-2	The mission shall include 2 to 6 12U spacecraft, launched on a single launcher, between 2022 and 2023.
MIS-3	Each spacecraft shall contain a camera, and either a LIDAR or a spectrometer. The measurements shall improve the ephemeris by an amount to be defined.
MIS-4	The mass budget per spacecraft, including margins, shall be limited to 24 kg.
MIS-5	The spacecraft volume shall be limited by the launcher envelope, considering that a maximum of 6 s/c with 6 upper stage shall be fitted inside this envelope.
MIS-6	Observation data shall be transmitted after each flyby. OBDH should allow the storage of all flyby data from both spacecraft in each flyby, for the full mission duration.
MIS-7	For dedicated launchers, cost per launch shall be limited to $100M (including all spacecraft, launcher, upper stage and operations).
MIS-8	The mission shall rely on Low Thrust Propulsion.
MIS-9	The mission lifetime shall be between 3 and 6 years.
MIS-10	The bus design process shall indicate which systems can rely on COTS components and which will require novel developments.
MIS-11	The mission must target multiple NEAs with diameter >50m, two of which must be >150m

Table 1: Mission requirements set for the concurrent design challenge

4. Mission Analysis

It is assumed that the spacecraft performs flybys of the asteroids at their nodal points; by remaining always on the ecliptic plane, the spacecraft can avoid expensive out-of-plane maneuvers. The correction maneuvers required to perform the flybys are realized using a low-thrust propulsion engine, whose thrust is inversely proportional to the square of the distance from the Sun. The thrust level at 1 AU is 3 mN, and the specific impulse of the engine is 3000s.

In order to determine the sequence of asteroids to visit, an initial analysis of the entire database of NEOs, available at [2], was performed. Later, the analysis was restricted only to asteroids with diameter greater than 50m. Considering the planetary defense context of the mission, only asteroids with diameter greater than 50 m are considered as potential targets. The diameter of the asteroids was estimated according to the relationship given in [12]. In this section, only the selected baseline solution with asteroids greater than 50m is presented. However, the mission analysis study included a complete analysis of the trajectory options for the years from 2023 to 2027, for all the asteroids in the database, and then for sequences of asteroids with diameter greater than 50 m, of which at least two greater than 150 m. It was found that for each considered launch window there exist several sequences of many NEOs that can be visited with a flyby at their nodal points. The length of these sequences can reach up to 15 asteroids for a three-year mission lifetime, if no constraints are imposed on the maximum total transfer time and on the minimum dimension of the visited asteroids.

In order to define the mission, the Minimum Orbital Intersection Distance [9,10] was computed between all the asteroids in the database, and different possible initial orbits of the spacecraft. The aim was to prune the search space by identifying asteroids for which the minimum distance from a

given initial spacecraft orbit was lower than 0.01 AU. The considered initial spacecraft orbits were characterized by apoapsis and periapsis in the range from 0.8 to 1.2 AU, to keep the spacecraft orbit close to the Earth's orbit. For non-circular orbits, the argument of the periapsis was allowed to vary in the range from 0 to 355 deg in steps of 5 deg. The inclination *i* and the right ascension Ω were kept equal to zero. This resulted in a total of 3240 possible initial orbits of the spacecraft. The analysis was later restricted to the combinations of values of r_a, r_p and ω for which the number of asteroids with MOID<0.01 AU was higher. The selected orbit has $r_a = 1.1$AU, $r_p = 1$AU and ω= 95 deg. At this stage, however, the selected orbit is characterized only by 5 orbital elements: *a, e, i,* Ω and ω. The next step in the definition of the mission is to define an initial mean anomaly for the spacecraft on its orbit, at a given initial time [5]; initial values of the mean anomaly in the range from 0 to 360deg were considered, and the considered initial dates (ie date of arrival on the initial orbit, not the launch date) ranged from the 1st of January 2023 to the 30th of December 2027, in intervals of 15 days. Launches before 2023 are considered, to allow for a 2023 start date of the initial orbit. This phasing analysis allowed checking which of the asteroids with MOID < 0.01 AU could actually be encountered [5]. The analysis of the phasing was then followed by a combinatorial analysis using a Binary Tree (BT). For each possible sequence of asteroids, the binary tree selected only those asteroids that are possible to visit with a total ΔV<2 km/s (not including transfer to initial S/C orbit), and for which the relative velocity at flyby is lower than 10 km/s. At this stage, the ΔV required to perform the flyby (that is, the ΔV required to go from distance<0.01AU, to distance equal to zero at the encounter), was estimated using an impulsive Lambert transfer between asteroids. Once the final solution was selected, all the transfers were optimized for low-thrust propulsion. In particular, the low-thrust trajectory was optimized to obtain the thrust profile that provides the minimum ΔV, using the toolbox FABLE (Fast Analytical Boundary-value Low-thrust Estimator), developed at the University of Strathclyde [4].

In the following, only the selected baseline solution that was considered for the rest of this paper is presented. Other solutions, visiting other asteroids, are available for all the considered initial dates for asteroids greater than 50m. It was found that for a start date in 2023 or 2025, solutions visiting 4 asteroids (two >150m) can be found. For 2024, up to 2 asteroids, both >150m, can be visited. In 2026 a solution with 3 asteroids (two >150m) was identified, while in 2027 a solution with 5 asteroids (two >150m) was found. Details about the selected baseline solution are given in Table 2. The table provides information about the low-thrust transfer to the initial orbit of the spacecraft, *OE*, and about the tour of the selected NEOs.

Transfer to $\mathcal{OE}$	
Launch date	22 December 2022
Arrival date on orbit $\mathcal{OE}$	30 January 2025
Transfer time to $\mathcal{OE}$	2 years, 1 month
ΔV to reach $\mathcal{OE}$ [km/s]	1.56
NEOs tour	
Start date for the tour of NEOs	30 January 2025
M_0 on $\mathcal{OE}$ on 30 January 2025 [deg]	325
Date of final flyby	8 August 2027
Total tour time	2 years and 7 months
ΔV to realise the tour [km/s]	0.7

Table 2: Details of the baseline solution considered for this work

Table 3 provides information about the asteroids in the baseline sequence, including the dates of encounters, the diameter of each asteroid, their semi-major axis, eccentricity and inclination, and the relative velocities at flyby.

SPK ID	Family	Date of encounter	Diameter [m]	*a* [AU]	e	*i* [deg]	Flyby rel. vel. [km/s]
3723829	Apollo	1/10/2025	70.756219	1.09	0.18	14.8	8.91
2508908	Aten	30/3/2026	223.750812	0.88	0.27	5.6	7.89
2010302	Amor	1/11/2026	467.481706	1.27	0.14	4.37	3.06
3802401	Aten	8/8/2027	70.756219	0.89	0.20	18.49	9.53

Table 3: Information on the visited asteroids

5. Flight Dynamics

The reference ephemerides used for the mission analysis are taken from [2]. Generally, these estimates are obtained using only a limited number of observations from Earth. Furthermore, this estimate is not updated regularly, mainly due to the high number of objects to track. Hence, the

resulting uncertainty should be taken into account in the mission and trajectory design phase for achieving successful visits of the asteroids. Table 4 shows the 1-σ uncertainty on the reference orbital elements [2] used for the trajectory design for the asteroids in the baseline concept.

SPK ID	Epoch	a [AU]	e [-]	i [deg]	Ω [deg]	ω [deg]	M [deg]
3723829	27/04/2019	1.3108e-4	1.2227e-4	1.0986e-2	1.8929e-3	1.5043e-2	0.24731
2508908	27/04/2019	1.3709e-9	9.1611e-8	7.6863e-6	9.7839e-6	1.7170e-5	2.3224e-5
2010302	27/04/2019	4.6220e-9	4.1186e-8	4.5070e-6	4.8595e-5	5.4414e-5	2.8506e-5
3802401	27/04/2019	1.0789e-05	4.4327e-4	8.0850e-2	5.7567e-3	5.0277e-2	0.10674

Table 4: 1- σ uncertainty on the visited asteroids' orbital elements

This knowledge uncertainty is tackled with a two-step approach:

1. The orbit determination (OD) step before the nominal flyby time. The spacecraft is tracked accurately from ground, whereas the asteroid is observed with the spaceborne camera. Combining these two measurements, the accuracy of the asteroid ephemeris will be improved significantly.
2. The correction step, in which the deviations between the nominal asteroid orbit, used for the reference trajectory, and the actual updated one are compensated through correction maneuvers.

While the actual ephemeris improvement approach will be discussed in Section 7.1, the remainder of this section will address two interconnected tasks: the quantification of the uncertainty at flyby, and the correction strategy once the asteroid has been targeted.

5.1 Asteroid Uncertainty at Flyby

To quantify the correction margins, the uncertainty on the asteroid ephemeris at the epoch time in Table 4 are propagated to the time of the nominal flyby. The resulting 3-σ ellipsoid on the position components is plotted for each asteroid in the baseline sequence in Figure 1 centered in the nominal asteroid position. The second and third asteroid in the sequence, whose ephemeris are well characterized due to their substantial size, have a rather low uncertainty at the flyby time. On the other hand, the smaller asteroids in the sequence, i.e. the first and last visited, are characterized by higher uncertainty which require higher delta-V correction margins. As this graph represents the 3-σ ellipsoids, the points on their surfaces may be considered the worst-case deviations to be compensated.

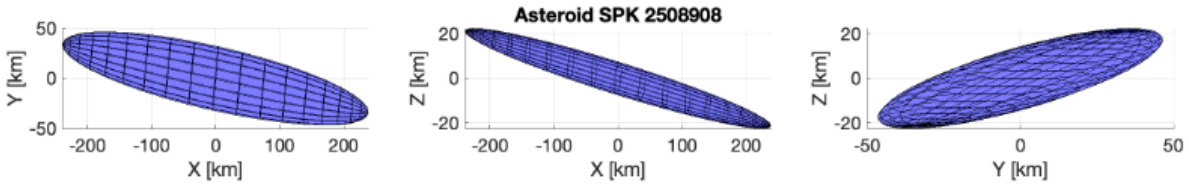

Figure 1: Example 3-σ ellipsoid of asteroid position at nominal flyby time centered at nominal position

5.2 Baseline Correction Strategies

Once the OD phase has pointed out the true asteroid orbit with acceptable accuracy, correction maneuvers should be performed to compensate the deviations between the reference and the actual asteroid position at flyby. Correction maneuvers can be performed by using the main low-thrust engine, or the high-thrust microthruster equipped for TCM, or a combination of the two. In terms of propellant expenditure, the optimal approach would be to employ mostly the more efficient low-thrust engine.

However, the deviations it can compensate in the arc of time between the orbit determination step and the flyby are bounded by its extremely low thrust level. Figure 2 shows the reachable sets of deviations around the nominal trajectory which are achievable by using low-thrust propulsion only. Each colored set corresponds to different numbers of days of thrust before the flyby. Depending on how soon the OD process and correction maneuvers are started, a greater region can be reached. Only the correction scenario for the first asteroid in the sequence is shown, as the graphs for the flyby with the other asteroids do not differ significantly, in spite of the different positions along the orbit. This is mainly due to the relatively small deviations and the short time arcs. Hence, the discussion hereafter applies to all flybys equivalently.

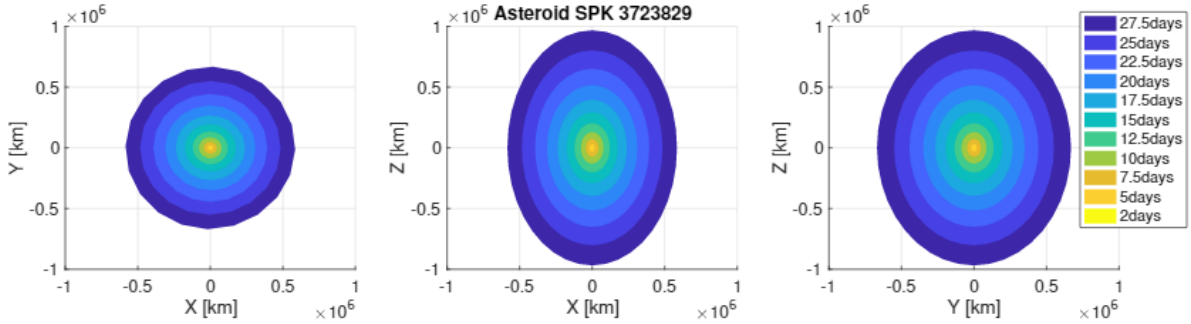

Figure 2: Set of deviations which are possible to compensate with low-thrust propulsion for different time intervals for the first flyby in the baseline sequence

By comparing Figure 1 with Figure 2, the minimum time before flyby to start the orbit determination and correction campaign can be assessed. For the second and third flyby in the sequence, the deviations are so small that they can be corrected in less than two days. For the first and last asteroid in the sequence, the worst-case deviations are larger than the low-thrust reachable set even when the orbit determination and correction phase starts almost one month before the flyby. When not reasoning for the worst-case scenario, the low-thrust engine is able to efficiently compensate most of the possible deviations for the asteroids as well.

It is possible to employ a combination of high-thrust and low-thrust correction to reach larger deviations. The optimal strategy is to fire the high-thrust engine at the beginning of the correction campaign, such that its effect can compound over time, before using the low-thrust engine.

If the actual deviation still exceeds any possible compensation margin, a close flyby (and hence mass measurement) will not be possible, however the primary objective or ephemeris improvement will still be achieved.

5.3 Operational Considerations

The actual asteroid orbit out of the uncertainty ellipsoids is available only after the operational OD, about 2 weeks pre-flyby. In terms of trajectory correction, the earlier the asteroid state is known accurately, the better. In the baseline trajectory there are ample time windows before the first flyby, and between the penultimate and final flybys, for long compensation maneuvers.

Finally, it is important to bear in mind that the flight dynamics considerations and strategies presented in this section highly depend on the current state of mission maturity and current level of knowledge of the asteroid ephemeris. In a realistic scenario, the asteroids ephemerides are expected to be updated from ground, but not necessarily improved, before the flybys. The update of the ephemeris to an epoch closer to the flyby date would result in smaller uncertainty ellipsoids as the effect of uncertain dynamical parameters decreases in smaller propagation windows.

6. Launch Vehicle Tradeoff and Upper Stage Feasibility Analysis

An initial database of launch vehicles was constructed from publicly available data on Wikipedia [3] and the manufacturers' websites. The initial database contained 108 vehicles (inc. variants), and listed properties such as typical payload delivery orbit (in LEO and in GEO, where applicable), the payload mass, date of first and last launch, country of origin, number of launches already performed, and where available, cost per launch and link to the user manual or more detailed datasheet. This initial list was then narrowed down to remove vehicles with incomplete data, those still in development with an expected launch date later than the mission, and those whose LEO payload is less than 200kg, which was derived from an early estimation of the mass of the kick stage required to bring a single 24kg spacecraft from LEO to an Earth escape trajectory. This narrowed the database down to 21 vehicles.

6.1 Piggyback Option

After consulting with the collaborators at ESA and JAXA, a piggyback option on a future mission was included. The most relevant and compatible mission found was the Euclid mission [11], which is expected to launch in June 2022 with a Soyuz 2.1b launch vehicle. Euclid will be launched to the Earth-Sun L2 point, which makes it compatible with NEACORE as this is equivalent to having an Earth escape with C3=0. Additionally, there was sufficient spare mass and volume in the payload to launch between 5 and 50 NEACORE satellites.

6.2 Dedicated Launch + Kick Stage Option

Of the 21 remaining vehicles, these were further narrowed down to 6. Of these, only the Falcon 9 is able to deliver a payload to an escape trajectory. In order to allow more flexibility in the choice of launch vehicle, the use of an upper stage to transfer to an interplanetary trajectory was considered.

A bottom-up design strategy was employed, first by looking at a list of viable engines. Then the possible payload mass (to the required C3) for each launcher initial orbit and engine combination was calculated, along with the required propellant mass. Engine masses are given, and the number was assumed to be equal to the number of carried satellites. Additional structural and electronics mass was assumed to be 50% of the sum of the mass of the tank and engines. The results of this analysis are shown in Table 5.

Vehicle	# S/C	Launch cost per spacecraft M$
Electron	1	6
LauncherOne	3	4
Skyrora XL	2	6
PSLV-CA	6	5.1
Epsilon	12	3.25
Falcon 9 FT (expended)	190	0.32

Table 5: Number of spacecraft that can be delivered to the required orbit by using a kick stage

The largest cost per spacecraft is never higher than $6M, and decreases if more spacecraft are launched together. However since these values assume that the launcher is used at full capacity, this means that even if the Falcon 9 results to be the cheapest on a per spacecraft basis, it is still the most expensive in total mission costs. Given that the total the total budget allowed for the mission is 100M$, this value might be too high, especially considering that is seems exceptionally unlikely that 190 NEACORE satellites will ever be used. All the other options instead seem much more plausible, both given the number of spacecraft launched, the cost per spacecraft, and the total launch cost in relation to the total budget. The final choice will depend on several other considerations, but this preliminary study should provide a robust basis for further developments.

7. Scientific Objectives and Measurement Strategy

The primary scientific objective was improvement of the targets' ephemerides by use of the navcam on approach and combining this with the relatively precisely known spacecraft position. It was concluded during the study that shape, size, albedo, rough surface features and possibly mass/density information could be obtained with the onboard instruments.

The satellite carries a time-of-flight LIDAR and a narrow-field dual-purpose science and navigation camera (COTS – SAC Chameleon Imager). The general concept of operations can be seen in Figure 3. This illustrates the previously discussed strategy of initial OD, trajectory correction, and close flyby.

Before the flyby, the spacecraft will determine their relative range using the radiolink and reduce relative velocity, before orienting themselves for LIDAR and camera measurements, and waiting for the target to pass through the field of view. After the flyby, the craft will return to measuring relative range and velocity in order to measure gravitational deflection. After all measurements are complete, the craft will transmit the processed data and cruise to the next burn point.

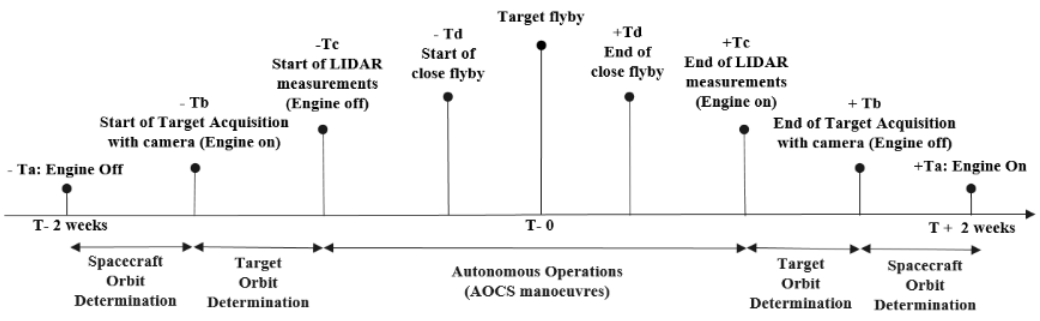

Figure 3: CONOPS for the Observation phase

7.1 Orbit Determination

Exposure requirements are calculated using the apparent magnitude of the object. Magnitude corrections of +0.7526 were made which assumes that the craft approaches at an angle such that approximately 50% of the target is illuminated. The total exposure time required for a given acquisition distance for each of the 4 asteroids in the studied tour, assuming the acquisition occurs at a distance from the sun equal to the targets' orbital semi-major axes as a worst-case, is shown in Figure 4.

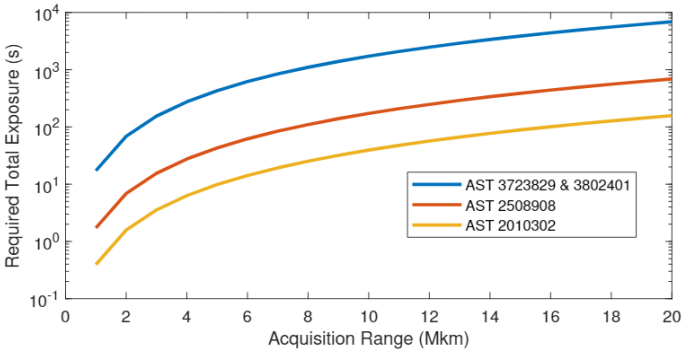

Figure 4: Required total exposure time to see each asteroid at a given distance pre-flyby. Note two have the same magnitude and thus curves are identical.

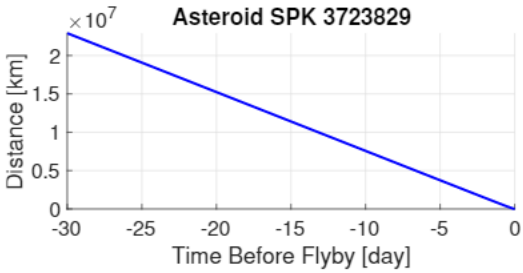

Figure 5: Distance between asteroid and spacecraft as a function of time pre-flyby

The threshold magnitude above which there are n_s stars in the camera FoV (expressed as the sky fraction τ) can be calculated according to

$$\frac{n_s}{\tau} = N_{ref}(2.5)^{m_{th}-m_{ref}}$$

Where N_{ref} is the number of stars in the entire sky brighter than magnitude m_{ref}. The chosen camera has a circular field of view with diameter 1.833°. In order to accurately track against background stars and obtain the asteroid's position, we assume there must be approximately 100 visible stars in the image. We calculate according to the above equation that there will be 100 stars in the FoV brighter than m_{th} = 12.08, which is significantly brighter than any of the targeted asteroids in our studied trajectory. Thus we can assume that if the exposure is long enough to detect the asteroid, there are more than sufficient background stars against which to track and determine position of the object.

The attitude control system chosen in the design study will be able to orient the spacecraft with a pointing error of ±0.0127° with a drift of <0.0318°s^{-1}. Over small timescales this can be assumed to be a linear drift . The camera has a per-pixel angular separation of $\Delta\varphi$=0.0011°, so if the image can be allowed to drift by two pixels during one integration (the camera will have some finite point spread function anyway so some blurring will have negligible effect), the maximum integration time can be calculated to be 69.2ms.

The observed position of the asteroid in relation to the expected position can be used to calculate a low-thrust trajectory correction maneuver which would be completed over the next several days in order to arrange a very close flyby (~50km) of the target. The two craft would fly in formation so as to fly by on opposite sides of the asteroid to enhance the gravitational trajectory deflection

7.2 Physical Characterization

Upon arrival, the LIDAR and science camera begin taking measurements. If the camera can take pictures of the asteroid while the LIDAR simultaneously measures the range, the shape and size can be determined by combining these two measurements. Due to high flyby velocities, the LIDAR will have a narrow time window during which it is inside its maximum operational range of the target. The spacecraft would align itself such that the LIDAR and camera point at some angle θ to the closest approach vector. The LIDAR begins emitting pulses in this direction, and waits for the asteroid to pass through the beam path, resulting in some pulses reflecting on the asteroid and being detected. If the LIDAR has a sufficiently high (~99%) probability for individual pulse detection, this will provide accurate measurements for the target range and also a secondary, independent method of determining the target dimensions by counting the number of returned pulses and combining with the known flyby velocity. The camera will also be active during the LIDAR measurement, operating in the same point-and-wait fashion (Figure 7). It would continually take pictures with a short exposure time

limited by motion blur. The maximum exposure time for no motion blur can be calculated by setting a limit that the object must not move by more than two adjacent pixels' angular separation during the integration time. The maximum integration time can be derived to be

$$t_{max} = \frac{d_{ca} tan(\Delta\phi)}{v_{flyby} cos^2(\theta)}$$

where d_{ca} is the measurement range from the asteroid, $\Delta\varphi$ is the angular resolution of the camera, v_{flyby} is the relative velocity at flyby and θ is the angle at which the optical measurement is taken relative to the closest approach vector. For the chosen camera, 40km closest approach, and flyby velocities of 7.89km/s and 3.06km/s, corresponding to the two largest asteroids in the studied mission, the tradeoff between transverse resolution and integration time per photo can be seen in Figure 6.

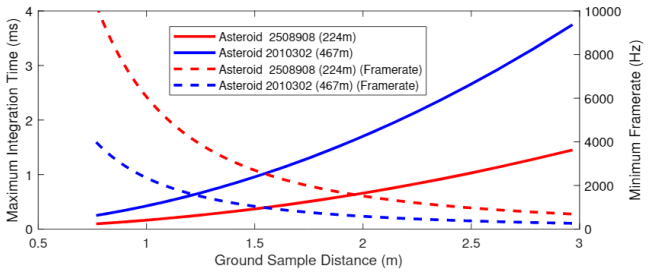

Figure 6: Tradeoff between observation distance and resultant GSD, and minimum required camera framerate for no-blur condition (solid lines for left y-axis)

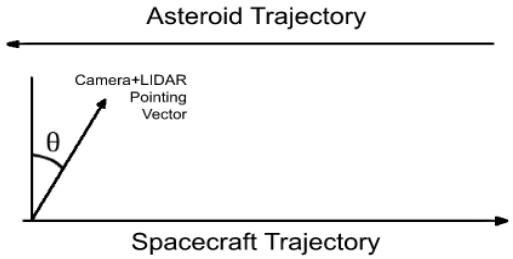

Figure 7: Illustration of instruments' pointing angle. Larger theta increases transit time and lowers framerate but necessitates larger camera GSD

The LIDAR has a maximum range of around 100km, which corresponds to a minimum GSD of approximately 1.9m, and minimum framerates around 600Hz and 1600 Hz for the two largest asteroids in the studied mission.

7.3 Mass Estimation Strategy

The asteroid mass is a critical quantity to estimate during an asteroid visit as it is extremely difficult to infer from ground observations. It is infeasible to reconstruct the asteroids' mass through ground observations of the spacecraft trajectory given the low deviation of a fast flyby with these small bodies, so local measurements must be used.

Exploiting the low cost per spacecraft of the proposed framework, a formation flying strategy has been devised to infer asteroids' mass. By employing two or more spacecraft in an advantageous geometrical configuration, intersatellite relative velocity changes become significantly more sensitive to the gravitational effects of the asteroid flyby. Intersatellite ranging measurements can then be employed to reconstruct the asteroid mass with better accuracy. Intersatellite ranging can be performed by two-way ranging (TWR) using either the radiolink or the LIDAR. In this method, one satellite sends an initial signal to be received by the second, which then re-transmits a second signal with known time delay to the first satellite. The delay can be used to infer the line-of-sight distance.

After the OD phase and correction maneuvers, the state of the two spacecraft is known with good accuracy. Small impulsive corrections are performed in order to maximally reduce spacecraft relative velocity and have them pass on opposing sides of the target to enhance gravitational relative deflection. During flyby, range measurements inform the closest approach distance. After flyby, intersatellite range measurements are collected for several days while the satellites are kept in the same configuration with respect to the Sun. By looking as deviations between actual measurements and those expected has the asteroid not been present,, a dynamic least-square can be employed to infer the asteroid mass.

Figure 8(a) shows an example of the jump in the relative velocity that appears during an asteroid flyby for different possible asteroid mass values. The value of this change is different for each visit mainly due to the different relative velocities at flyby. The effect builds up over time (Figure 8(b)), and therefore range measurements become detectable via two-way ranging (TWR) with ISL or possibly the onboard LIDAR systems (also using TWR).

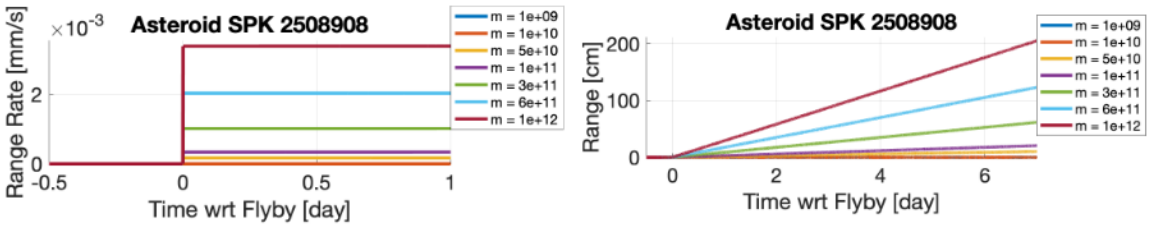

Figure 8: (a) relative velocity shift due to flyby (b) relative position evolution post-flyby

This shows that asteroid mass can be inferred by measuring the range drift after the flyby. The dynamic least-square fit run to process the acquired data would then provide a precise best estimate for the mass value and an associated uncertainty measure.

The first and last asteroids in the studied tour are likely too small to yield measurable disturbance on the spacecraft trajectory, however the collected measurements in combination with size and shape information could be used to better bound the asteroid mass and density.

8. Mission Cost and Sustainability Assessment

8.1 Overview

Life Cycle Sustainability Assessment (LCSA) was included as a mandatory discipline within the NEACORE concurrent design study. LCSA is a new environmental management methodology used to measure the environmental, social and economic impact of products, processes and services over their entire life cycle. It allows an assessment of products to be made based on the traditional 'three pillar' interpretation of sustainability by combining Environmental Life Cycle Assessment (E-LCA), Social Life Cycle Assessment (S-LCA) and Life Cycle Costing (LCC). Therefore, LCSA is a framework of models designed to provide more relevant results in the context of sustainability and allow integrated decision-making based on a life cycle perspective.

8.2 Goal & Scope Definition

The primary objective of the LCSA discipline within the NEACORE study was to identify and minimize adverse environmental, social and economic impacts of the entire mission without significantly compromising technical aspects. The LCSA was modeled following the procedures outlined in [13,14,15,16,17,18,19,20,21,22]. The generated results are relevant for 6 spacecraft (including system and subsystem mass margins) launched on a dedicated PSLV-CA in 2022 for a mission duration of 4 years and 8 months. Based on this mission definition, the functional unit was determined to be 'the NEACORE mission in fulfillment of its requirements' for a system boundary covering all activities during each mission phase as outlined in [13].

8.3 Life Cycle Inventory Analysis

The data used in this study came directly from information deposited to CDP-4 during the concurrent design session, expert knowledge and domain-specific default values. This information was input to the Strathclyde Space Systems Database (SSSD) which formed the life cycle inventory (LCI). Its LCI contains a total of 410 custom-made space-specific processes which are supported by the European Life Cycle Database version 3.2 and Ecoinvent versions 2.2 and 3.3 as background databases. Each LCI dataset has environmental and costing data included, with an option to also add social criteria as well (since the SSSD does not currently have inventory data relating to social aspects).

8.4 Life Cycle Impact Assessment

The SSSD was also used for the life cycle impact assessment (LCIA). For E-LCA, the applied method is based on the recommended midpoint-level environmental impact categories and their calculation sources outlined within the ESA LCA guidelines [13]. Midpoint-level is a problem-oriented approach which translates impacts into themes such as climate change, ozone depletion, air acidification, human toxicity, etc. Additionally, newly developed S-LCA and LCC LCIA impact categories were also used for social and costing results. Further information on these methodologies can be found in the SSSD user guide [23]. The results of each of these assessments are provided on the next page, including social and costing aspects as E-LCA single score impact categories.

When looking at the E-LCA, the impact categories of climate change, freshwater aquatic ecotoxicity, human toxicity, mineral resource depletion and ozone depletion were selected for further

investigation since they were identified by ESA's Clean Space Initiative as being 'hotspots' for space missions [24]. In this context, it was found that the manufacturing and production of the launcher and its propellant were jointly responsible for the majority of the climate change and freshwater aquatic ecotoxicity impacts whilst the launch event contributed 99.99% of the ozone impact, mainly due to ClOx, HOx, NOx and HCl compound releases from the combustion of the solid propellant. The spacecraft solar arrays alone produced 99.77% of the human toxicity impact due to dioxin releases during manufacturing and production of the germanium substrate. Germanium was also responsible for 99.01% of the mineral resource depletion impact.

In terms of S-LCA, only the stakeholder categories of workers and value chain actors (VCAs) were investigated. Overall, it was found that 85.94% of total impact rose during Phase C+D due to the number of VCAs involved in production and manufacturing of the craft. It was found that the VCA stakeholder subcategories of fair completion (15.12%) and supplier relationships (15.02%) scored highest amongst all 13 stakeholder subcategories. This was because many of the VCAs country of operation were ones in which there has been evidence of anti-competitive behavior and are also more likely to breach competition laws in addition to inconsistencies regarding payment to suppliers and sufficient lead times at national level.

As one of the main mission objectives of the NEACORE study was to keep the cost as low as possible, LCC played a particularly important role. It was found that the total cost of the mission would be 2.97E+07 EUR 2000 of which around 69% is directly attributable to the acquisition cost of the launcher and around 20% due to ground operations. When this is converted into present value USD then the result is 4.49E+07 USD 2019. Additionally, since the mission is for commercial purposes then two business models can be applied to account for revenues. In the first, the organizing body would be responsible for all costs over the mission life cycle and sells to customer with a 20% profit margin. In the second, the organizing body would be responsible for all costs up to (and including) the launch and sells to customer with a 20% profit margin. The customer would therefore be responsible for operation and end of life costs. These are outlined below along with the associated costs to the customer:

(a) Business Model A

Cost element	Cost per 6 spacecraft	Cost per spacecraft
Whole mission	$44,878,328.12	$7,479,721.36
20% profit margin	$8,975,665.62	$1,495,944.27
Total cost	**$53,853,993.75**	**$8,975,665.63**

(b) Business Model B

Cost element	Cost per 6 spacecraft	Cost per spacecraft
Up to and incl. launch	$33,963,918.72	$5,660,653.12
20% profit margin	$6,792,783.74	$1,132,130.63
Total cost	**$40,756,702.46**	**$6,792,783.75**

Table 6: Cost per Spacecraft based on business models

It is worth noting that the cost per spacecraft could be reduced even further if more were to be launched on-board the PSLV. However, these values do not take into consideration environmental remediation costs due to the environmental impact of the mission. It would cost an additional $200,605.44 to offset the CO_2e emissions released from this mission alone based on the UK Government's Carbon Price Floor [25]. This equates to $33,434.24 per spacecraft.

8.5 Multi-Criteria Decision Analysis

Although each of these assessments can be viewed as standalone results, in order to gauge how the three sustainability dimensions interact with one another, Multi-Criteria Decision Analysis (MCDA) was applied using the Multi-Attribute Value Theory method. In this regard, MCDA is used to come to a single environmental score and single sustainability score in order to compare the three sustainability dimensions using the following weighted sum formula:

$$v(a) = \sum_{i=1}^{I} w_i v_i(a)$$

Where $v(a)$ is the overall sustainability score of product a, w_i is the weighting factor for impact category i, $v_i(a)$ is the score reflecting the performance of product a on impact category i, and I is the total number of impact categories.

For E-LCA, normalization and weighting applied was based on [26, 27] which converted the results of the 5 'hotspot' impact categories into a single environmental score measured in impact magnitude per EU citizen annually. New normalization methods were used for S-LCA and LCC as detailed in [23] which was based on the total annual European organizational social score per EU citizen and average EU-28 tax paid per EU citizen. Weighting was not necessary for either S-LCA or LCC since they were already in the form of a single score. However, to come to an overall sustainability score, MCDA can be applied using the normalized and weighted single scores of each

sustainability dimension as the sustainability score. The applied weighting factors are based on research by [28] which identified the percentage of Sustainable Development Goals and their associated targets which focus on environmental (18%), social/governance (53%) and economic (29%) issues. The LCSA results of the NEACORE mission were generated using this method which can be seen in the appendix (Fig 11). This technique is explained in further detail in the SSSD user guide [23].

Overall the results show that the environmental impacts are the most problematic of the three sustainability dimensions for the mission, contributing 89.26% of the single score sustainability impact. This is primarily due to the launch vehicle and the use of germanium as a substrate in the solar array. For this reason, the environmental impacts were the most closely monitored with efforts made to lowering them as far as practically possible. Some of the ecodesign options considered included reducing the solar array size and switching the AOCS propellant from argon to AF-M315E which is a high performance green propellant. As such, the solar array was reduced by 32.78% leading to vast single score environmental savings. However, it was found that the switching of propellants offered no significant environmental benefits. Additionally, the observable decrease between iteration 1 and 2 was due to more relevant data becoming available. The increase in environmental results from iteration 2 and 3 was due to a change in launchers for commercial reasons (from a Soyuz 2-1b piggy-back assuming a 20% share in environmental, social and economic impact to a dedicated PSLV-CA launcher). Despite this change, the savings from the solar array limited the overall environmental score from increasing beyond the score of iteration 1.

8.6 Interpretation

This was the first study to successfully integrate E-LCA, S-LCA and LCSA fully into the concurrent design process of a space mission worldwide, highlighting the usefulness of the discipline in determining adverse sustainability impacts during the concurrent design process and providing solutions to lower them.

The main limitations of this study stemmed from the generalization and/or omission of certain LCI datasets from the SSSD due to their uniqueness (e.g. LIDAR) which meant that a best fit had to be chosen instead. Furthermore, since the SSSD also does not contain an S-LCA LCI, social impacts were measured at country-level which does not accurately reflect relevant stakeholders. Additionally, estimates for cost of operations ranged from $750 to €1,500 per hour. This uncertainty meant that the total cost of operations for 6 spacecraft varied from $5.292M to $11.854M including a 20% margin. For this reason, a conservative cost estimation of $960 per hour was applied based on NASA's Deep Space Network (DSN) published formula, leading to a total cost of $7.292M [29]. Finally, normalization and weighting applied during LCSA adds subjectivity to the outcome of the analysis. In particular, the E-LCA single score only considers certain hotspot impact categories which may obscure results.

Based on these findings and limitations, the following recommendations were set out by the LCSA discipline for future NEACORE design sessions:

- Launcher trade-offs should take place based on the environmental impact.
- The feasibility of using solar panels without germanium substrates should be examined.
- S-LCA should investigate impacts at an organizational level with stakeholder participation.
- Cost of operations needs to be more accurately estimated.
- Single score results should not be solely relied upon and should only be used as a guide.

9. Concurrent Engineering Study Results and Conclusions

As mentioned in the introduction, the mission concept presented in this paper results from a one-week feasibility study led at the CCDS of the University of Strathclyde. The team was composed of 16 PhD students from the Departments of Mechanical & Aerospace Engineering and Electronic & Electrical Engineering who worked together in a concurrent engineering environment. The study process went through 3 design iterations, the final configuration and mass budget are detailed in this chapter. The simultaneous update and exchange of parameters relied on an open-source software developed by RHEA Group, the Concurrent Design Platform, CDP4-Community Edition.

A CAD drawing of the final design configuration can be seen in Figure 9. An effort was made to adhere to a 12U CubeSat form factor and a CubeSat frame was used. Although not strictly necessary, this further simplifies and cheapens the production and launch costs due to COTS CubeSat component availability, and adds a level of flexibility as piggybacking on another launch will still be a possibility. Solar panels are oriented such that they can be in full sunlight during burns as all thrust vectors are aligned with the solar orbital prograde vector. The high gain antenna is oriented pointing 'forward' as during the majority of the considered mission the Earth will be closest to this orientation, and attitude control can make orientation adjustments to communicate with Earth.

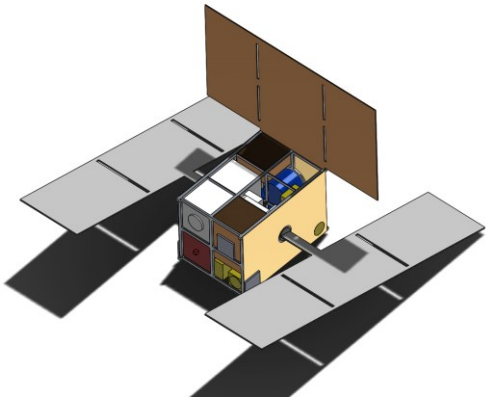

Figure 9: Final NEACORE Configuration. An effort was made to adhere to 12U stowed configuration

The final mass breakdown including subsystem and system margin, is displayed in Table 7. The majority of the components chosen during the Concurrent Engineering study were COTS. However, the kick stage and the LIDAR will require new developments. A miniaturized ToF LIDAR system is currently under development at the University of Strathclyde in collaboration with Fraunhofer UK with this mission concept in mind, and will be using the SWaP budgets and range requirements from this study as performance targets. Additionally to this, the large deployable solar panels and reflectarray antenna are not COTS options – however they are based on similar components used in the M-ARGO design.

Subsystem	Mass (inc. margins) [kg]	Percentage of Dry Mass [%]
Structure	2.75	13.65
AOCS	3.2	15.9
Mechanisms	0.59	2.92
OBDH	0.37	1.82
Power	2.54	12.6
Propulsion	3.42	17
TT&C	2.48	12.31
Thermal	1.56	7.74
Harness	0.55	2.73
Instruments	2.96	13.35
Total Dry Mass	20.14	without 10% system margin
Total Dry Mass (with margin)	22.15	with 10% system margin
Total Wet Mass (with margin)	23.74	with 1.59 kg fuel (incl. 2% margin)

Table 7: Mass Breakdown from Design Study

9.1 Conclusions

During this Concurrent Engineering study a satellite platform and mission framework was successfully designed that fulfills all mission requirements laid out in section 3.A detailed analysis of one specific target set was performed to assess the feasibility of measurements at high flyby velocities. It was deemed possible to achieve the primary objective of ephemeris improvement, and also to take all secondary measurements and to be able to resolve surface details with resolution of approximately 6m (double the achievable GSD). The framework presented provides a feasible method for low cost large scale exploration of large numbers of NEAs, particularly in the case of dedicated launches using for example the PSLV-CA or Epsilon launchers as this keeps the cost per spacecraft low and the potential number of visited objects high. Additionally, the mass and size were kept within 12U CubeSat limitations which allows for this framework to be applied to piggyback options as well as dedicated launchers.

References

[1] Auxiliary passengers user guide 1.0

[2] JPL small-body database search engine

[3] Wikipedia: Comparison of orbital launch systems

[4] Marilena Di Carlo, Juan Manuel Romero Martin, and Massimiliano Vasile. Camelot: computational-analytical multi-fidelity low-thrust optimization toolbox. CEAS Space Journal,10(1):25–36, 2018

[5] Marilena Di Carlo,Massimiliano Vasile, and Jamie Dunlop. Low-thrust tour of the main belt asteroids. Advances in Space Research, 62(8):2026–2045, 2018.

[6] E. Woeppel et. Al. The near earth object scout spacecraft: A low-cost approach to in-situ characterization of the near earth object population. 05 2014.

[7] Franco Perez et. Al. Dustcube, a nanosatellite mission to binary asteroid 65803 Didymos as part of the ESA AIM mission. Advances in Space Research, 62(12):3335 – 3356, 2018. Advances in Technologies, Missions and Applications of Small Satellites.

[8] Cristian Greco, Marilena Di Carlo, Lewis Walker, and Massimiliano Vasile. Analysis of NEOs reachability with nano-satellites and low-thrust propulsion. 06 2018.

[9] Giovanni F Gronchi. On the stationary points of the squared distance between two ellipses with a common focus. SIAM Journal on Scientific Computing, 24(1):61–80, 2002.

[10] Giovanni F Gronchi. An algebraic method to compute the critical points of the distance function between two keplerian orbits. Celestial Mechanics and Dynamical Astronomy, 93(1-4):295–329, 2005.

[11] Rene Laureijs, J Amiaux, S Arduini, J-L Augueres, J Brinchmann, R Cole, M Cropper, C Dabin,L Duvet, A Ealet, et al. Euclid definition study report. arXiv preprint arXiv:1110.3193, 2011.

[12] Edward F Tedesco. Iras minor planet survey. In Symposium-International Astronomical Union, volume 160, pages 463–466. Cambridge University Press, 1994.

[13] European Space Agency LCA Working Group, “Space system Life Cycle Assessment (LCA) guidelines,” 2016.

[14] International Organization for Standardization, *ISO 14040:2006 Environmental management – Life cycle assessment – Principles and framework,* Geneva, Switzerland, 2006.

[15] International Organization for Standardization, *ISO 14044:2006 Environmental management – Life cycle assessment – Requirements and guidelines,* Geneva, Switzerland, 2006.

[16] European Commission, “Product Environmental Footprint Category Rules Guidance,” 2018.

[17] United Nations Environment Programme and Society of Environmental Toxicology & Chemistry, “Guidelines for Social Life Cycle Assessment of Products,” Paris, France, 2009.

[18] United Nations Environment Programme and Society of Environmental Toxicology & Chemistry, “The Methodological Sheets for Subcategories in Social Life Cycle Assessment (S-LCA),” Paris, France, 2013.

[19] International Organization for Standardization, *ISO 26000:2010 Guidance on social responsibility,* Geneva, Switzerland, 2010.

[20] UN General Assembly, “Transforming our world : the 2030 Agenda for Sustainable Development,” 21 October 2015, A/RES/70/1.

[21] International Electrotechnical Commission, *IEC 60300-3-3:2017 Dependability management Part 3-3: Application guide – Life cycle costing,* Geneva, Switzerland, 2017.

[22] United Nations Environment Programme and Society of Environmental Toxicology & Chemistry, “Towards a Life Cycle Sustainabiulity Assessment,” Paris, France, 2011.

[23] A. R. Wilson, “Strathclyde Space Systems Database User Guide – Version 1.0.0,” Glasgow, UK, 2019.

[24] S. Morales, Interviewee, *Personal Commuication with European Space Agency Ecodesign Expert.* [Interview]. 7 April 2019.

[25] D. Hirst, “Carbon Price Floor (CPF) and the price support mechanism,” House of Commons, London, UK, 2018.

[26] L. Benini, L. Mancini, S. Sala, S. Manfredi, E. M. Schau and R. Pant, “Normalisation method and data for Environmental Footprints,” European Commission, Joint Research Center. Institute for Environment and Sustainability. Publications Office of the European Union, Luxembourg, 2014.

[27] S. Sala, A. K. Cerutti and R. Pant, “Development of a weighting 7pproach for the Environmental Footprint,” European Commission, Joint Research Center. Institute for Environment and Sustainability. Publications Office of the European Union;, Luxembourg, 2018.

[28] J. Martínez-Blanco, A. Lehmann, Y.-J. Chang and M. Finkbeiner, “Social Organizational LCA (SOLCA) – a new approach for implementing social LCA,” *International Journal of Life Cycle Assessment,* vol. (2015), no. 20, pp. 1586-1599, 2015.

[29] National Aeronautics and Space Administration, “NASA’s Mission Operations and Communication Services,” 1 October 2014. [Online]. Available: https://deepspace.jpl.nasa.gov/files/6_NASA_MOCS_2014_10_01_14.pdf. [Accessed 17 May 2019].

[30] Selva, D. and Krejci, D., 2013. Preliminary Assessment of Performance and Cost of a Cubesat Component of the Earth Science Decadal Survey.

[31] Benedetti, G., Bloise, N., Boi, D., Caruso, F., Civita, A., Corpino, S., Garofalo, E., Governale, G., Mascolo, L., Mazzella, G. and Quarata, M., 2019. Interplanetary CubeSats for asteroid exploration: Mission analysis and design. *Acta Astronautica*, *154*, pp.238-255.

[32] Goel, A., Krishnamoorthy, S., Swenson, T., West, S., Li, A., Crew, A., Phillips, D.J., Screve, A. and Close, S., 2017. Design for CubeSat-based dust and radiation studies at Europa. *Acta Astronautica*, *136*, pp.204-218.

[33] Viscio, M.A., Viola, N., Corpino, S., Stesina, F., Fineschi, S., Fumenti, F. and Circi, C., 2014. Interplanetary CubeSats system for space weather evaluations and technology demonstration. Acta Astronautica, 104(2), pp.516-525.

APPENDIX

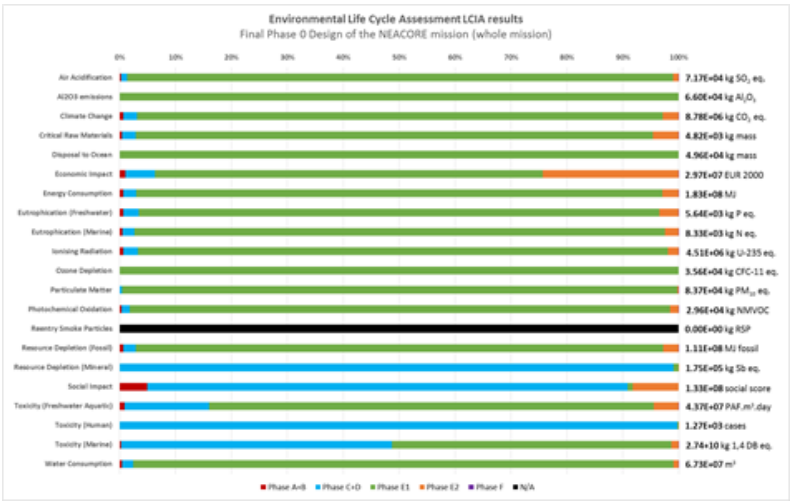

Figure 10: Life Cycle Impact Assessment Results of the NEACORE Mission

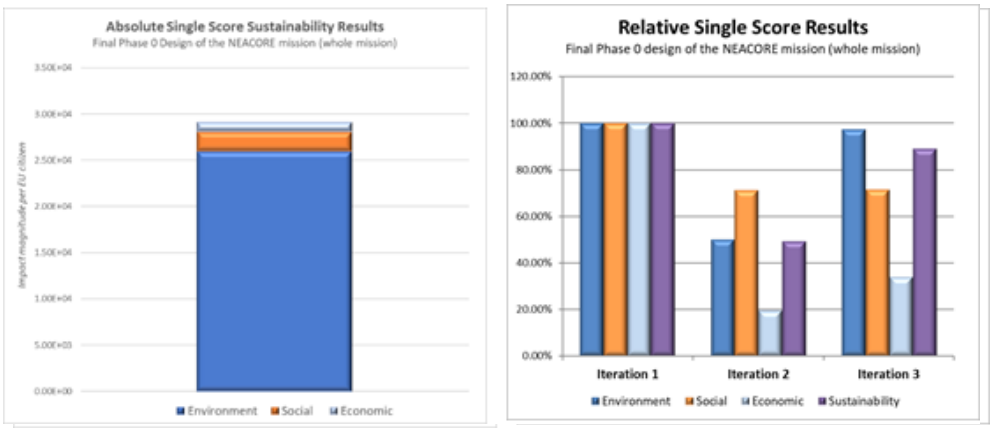

Figure 11: Life Cycle Sustainability Results of the NEACORE mission.
(a) Absolute Results, (b) Relative Results